Time-Resolved Monitoring of Flash-Induced Changes of Fluorescence Quantum Yield and Decay of Delayed Light Emission in Oxygen-Evolving Photosynthetic Organisms†

R. Steffen, G. Christen, and G. Renger*

Max-Volmer-Institut für Biophysikalische Chemie und Biochemie, Technische Universität Berlin, Strasse des 17. Juni 135, 10623 Berlin, Germany

Received May 24, 2000

ABSTRACT: The present contribution describes a new experimental setup that permits time-resolved monitoring of the rise kinetics of the relative fluorescence yield, $\Phi^{rel}(t)$, and simultaneously of the decay of delayed light emission, $L(t)$, induced by strong actinic laser flashes. The results obtained by excitation of dark-adapted samples with a train of eight flashes reveal (a) in suspensions of spinach thylakoids, $\Phi^{rel}(t)$ exhibits a typical period four oscillation that is characteristic for a dependence on the redox states S_i of the water oxidizing complex (WOC), (b) the relative extent of the unresolved "instantaneous" rise to the level $\Phi^{rel}_{rise}(100\ ns)$ at 100 ns and the maximum values of $\Phi^{rel}(t)$ attained at about 45 μs after each actinic flash, $\Phi^{rel}_{m}(45\ \mu s)$ synchronously oscillate and exhibit the largest values at flash nos. 1 and 5 and minima after flash nos. 2 and 3, (c) opposite effects are observed for the normalized extent of the rise kinetics in the 100 ns to 5 μs time domain of relative fluorescence yield, $\Phi^{rel}(5\ \mu s) - \Phi^{rel}(100\ ns)$, i.e., both parameters attain minimum and maximum values after the first/fifth and second/third flash, respectively, and (d) analogous features for the "fast" and "slow" ns-kinetics of the fluorescence rise were observed in suspensions of *Chlamydomas reinhardtii* cells. A slight phase shift by one flash is ascribed to physiological differences. The applicability of this noninvasive technique to study reactions of photosystem II, especially the reduction kinetics of $P680^{\bullet+}$ and their dependence on the redox state S_i of the WOC, is discussed.

Excitation energy transfer and trapping in photosynthesizing organisms inevitably comprises loss reactions. Among these, radiative emission from chlorophylls giving rise to red fluorescence offers an invaluable analytical tool to study the dynamics and efficiency of the primary processes of photosynthesis. These methods are especially suitable for studying photosystem II (PS II)[1] because most of the emission originates from PS II (for reviews, see refs *1* and *2*). The kinetics of trapping reactions leading to "stabilized" charge separation in form of the radical pair $P680^{\bullet+}PheoQ_A^{\bullet-}$ can be analyzed by time-resolved measurements of the decay kinetics of prompt fluorescence (see ref *3* and references therein). Single photon counting technique is most widely used for this type of measurements. The samples are excited with very weak laser flashes thereby avoiding interfering effects owing to annihilation phenomena (*4*). Recent technical developments permit simultaneous measurements in the time and frequency domain (*5*). The state $P680^{\bullet+}PheoQ_A^{\bullet-}$ is formed within 1 ns (*6*−*8*). Information on the rate of the subsequent redox reactions energetically driven by $P680^{\bullet+}$ and $Q_A^{\bullet-}$ can be gathered from analyses of the time course of the relative fluorescence quantum yield, $\Phi^{rel}(t)$, because $P680^{\bullet+}$ acts as a nonphotochemical quencher (*9*) and Q_A as photochemical quencher (*10*). Accordingly, the reduction of $P680^{\bullet+}$ is coupled with an increase of $\Phi^{rel}(t)$ and the reoxidation of $Q_A^{\bullet-}$ gives rise to a decrease of $\Phi^{rel}(t)$. As a consequence, the recombination reaction between $P680^{\bullet+}$ and $Q_A^{\bullet-}$ does not change $\Phi^{rel}(t)$, and only the kinetics of the separate reactions of both species can be monitored through measurements of $\Phi^{rel}(t)$ (for a more detailed discussion, see ref *11*). The kinetics of $P680^{\bullet+}$ reduction strongly depends on the integrity of the water-oxidizing complex (WOC). In samples fully active in oxygen evolution, $P680^{\bullet+}$ is reduced by the redox active tyrosine Y_Z via a multiphasic kinetics with dominating reactions in the ns time domain (*12*, *13*). The fast reduction requires an intact hydrogen bond between the OH group of Y_Z and a nearby base (*13*, *14*) identified as His 190 of polypeptide D1 (*15*). The microsecond-kinetics reflect relaxation processes within a hydrogen bond network that shift the equilibrium ($P680^{\bullet+}Y_Z \rightleftharpoons P680Y_Z^{ox}$) toward the right side. The normalized extent of the different kinetic components is a function of the redox states S_i of the WOC (*11*−*14*, *16*). After destruction of the WOC, the $P680^{\bullet+}$ reduction is dominated by a pH dependent kinetics in the range of 1−20 μs (*17*, *18*). $Q_A^{\bullet-}$ becomes reoxidized by a second plastoquinone molecule (Q_B) noncovalently bound to a special pocket (Q_B site). The kinetics (150−600 μs) of

† The financial support by Deutsche Forschungsgemeinschaft (Re 354/17-4) is gratefully acknowledged.

* To whom correspondence should be addressed.

[1] Abbreviations: Car, carotenoids; Chl, chlorophyll; fwhm, full width at half-maximum; MCP-PMT, microchannel plate photomultiplier tube; MES, morpholinoethane sulfonic acid; Pheo, pheophytin; P680, photoactive chlorophyll of PS II; PS II, photosystem II; Q_A, primary quinone acceptor of PS II; WOC, water-oxidizing complex.

10.1021/bi0011779 CCC: $20.00
Published on Web 12/05/2000

these electron-transfer steps depend on the redox state of Q_B (*19*, *20*). This brief description shows that the reactions of $P680^{\bullet+}$ and $Q_A^{\bullet-}$ are kinetically separable and therefore in principle the reduction of $P680^{\bullet+}$ and reoxidation of $Q_A^{\bullet-}$ can be monitored by the rise and decay, respectively, of $\Phi^{rel}(t)$. To achieve a significant population of $P680^{\bullet+}$ and $Q_A^{\bullet-}$ the samples have to be excited with actinic flashes of sufficiently high photon density. This, however, gives rise to a strong prompt fluorescence that severely affects the detector system. Therefore, artifacts due to this phenomenon have to be eliminated. This goal has been reached for a time range longer than a few microseconds after the actinic flash. Commercially available high-frequency modulated chlorophyll fluorometers as described in ref *21* are available. Accordingly, the analysis of $Q_A^{\bullet-}$ reoxidation via $\Phi^{rel}(t)$ is a widely used method that permits noninvasive investigations in whole algae and leaves of higher plants (see ref *22* and references therein). However, problems arise for studies of $P680^{\bullet+}$ reduction in the submicrosecond time domain, especially if the dependence on the redox state S_i of the WOC is studied. In this case actinic laser flashes of sufficient energy have to be used in order to minimize the damping of the S_i state cycle (for a review, see ref *23*). As a consequence, the distortion of the detector by the prompt fluorescence is rather strong, and its elimination at a short time after the actinic flash requires rapid gating with a sufficiently high switching ratio. This is a difficult problem, and to the best of our knowledge, except of one previous report using a probe pulse of comparatively high intensity (*24*), the time resolution was restricted by a "dead time" of $0.5-1$ μs (see ref *25* and references therein). The development of a new generation of multichannel plate (MCP) detector units with very fast gating at high switching ratios opened a new road for improving the time resolution of $\Phi^{rel}(t)$ measurement. This communication describes an equipment that not only permits monitoring of $\Phi^{rel}(t)$ but also of delayed light emission down to 100 ns after strong actinic flashes. Examples for the application of this method are presented.

MATERIALS AND METHODS

Sample Material. Thylakoid membranes were isolated from local market spinach as described by Winget et al. (*26*). All measurements were performed at room temperature in a pH 6.5 buffer medium (50 mM MES and 10 mM NaCl) with a chlorophyll concentration of 10 μg/mL. *Chlamydomonas reinhardtii* was grown in a TAP medium at a temperature of 27 °C as outlined in ref *27*. Measurements of cell suspensions were performed in the growth medium with a chlorophyll concentration that gives rise to nearly the same F_O level as for thylakoid suspensions.

Equipment. The sample in the cuvette is excited by actinic flashes ($\lambda = 532$ nm and fwhm = 10 ns) from a frequency-doubled Nd:YAG laser (Spectrum GmbH) at a repetition rate of 1 Hz. The essential progress in improving the time resolution was achieved by using the multichannel plate photomultiplier tube (MCP-PMT) R5916U-51 from Hamamatsu that permits a rapid gating of the detector. It contains a red sensitive photocathode (multialkali element) and can be gated with $\tau \approx 1$ ns and a high switching ratio of 1.7×10^8 (at $\lambda > 500$ nm). The time course of flash-induced changes of the relative fluorescence quantum yield is obtained by monitoring the fluorescence emission caused by the weak measuring light beam supplied by two arrays each containing seven LED's (Toshiba TLRA 190 P, $\lambda_{max} = 660$ nm).

The measuring system is controlled by a computer that is equipped with a National Instruments PC-TIO-10 timing and digital I/O interface. The I/O board is programmed to gate a pulse generator that triggers the frequency doubled Nd:YAG-laser. For synchronization with the gate function of the MCP-PMT, the Q-switch of the laser system is retarded by a delay/pulse generator (Stanford Research Systems, DG535). The delay time for the Q-switch is adjusted to obtain a maximum laser pulse energy of about 1.1 mJ/pulse and per unit area (1 cm^2). In parallel with the Q-switch the delay/pulse generator triggers a function generator (Stanford Research Systems, DS345) in such a way that the MCP-PMT is switched on 100 ns after the laser flash. Due to technical limits of the function generator, the gate function has a jitter of about 20 ns. The gate function for the MCP-PMT is amplified to a suitable voltage level by a pulse generator (Systron-Donner Corporation, Datapulse, rise time about 5 ns). The gate function is specifically selected in order to permit the monitoring of fluorescence signals by the MCP-PMT within three different time regions with respect to the laser flash. The F_0 level is determined in a time range from 2.4 to 0.8 μs prior to sample excitation with the actinic laser flash. The flash-induced rise kinetics of the fluorescence $F(t)$ and its maximum level F_m are recorded within time windows ranging from 0.1 to 5 μs and 43 to 46 μs, respectively, after the actinic laser pulse. The LED arrays providing the weak measuring light are switched on and off synchronously with the gate function of the MCP-PMT via the delay/pulse generator. The pulse generator (Systron-Donner Corporation, Datapulse) which triggers the switch (for a general description, see ref *25*) for the LED's voltage supply is used in double pulse mode to achieve two separate LED-pulses for the time regions from 4 μs before to 6 μs after the laser pulse, and from 41 to 48 μs after the laser pulse. A small fraction of the laser beam is focused on a photodiode by means of a beam splitter. The output signal of this photodiode triggers the data acquisition of the digital storage oscilloscope (Tektronix TDS 520) with an electrical band width of 100 MHz. The adjustment to optimum intensities and spectral properties of actinic and monitoring light beams is achieved by using combinations of optical filters. A scattering glass is placed in front of the sample cuvette to obtain a homogeneous illumination of the whole sample volume (approximately 1 mL). The photon density of the actinic laser pulses hitting the sample cuvette is adjusted via neutral glasses (NG 5, Schott) to avoid oversaturation of the sample. The fluorescence emission collected at an angle of 90° with respect to the incident laser beam is passed through a 532 nm laser blocker and funneled into the MCP-PMT detector unit by means of a light guide. For measurements of the changes of the fluorescence quantum yield a combination of a 730 nm interference filter and a 685 nm long-pass filter (Omega Optical Inc.) was used to separate the fluorescence signal from the measuring light. Signal amplitudes were adjusted to a range between 1 and 20 mV by placing neutral glasses (NG 5, Schott) before the MCP-PMT in order to avoid detector saturation. The measuring light of the LED array is passed through a cutoff filter ($\lambda < 700$ nm, Balzer DT Cyan Spezial).

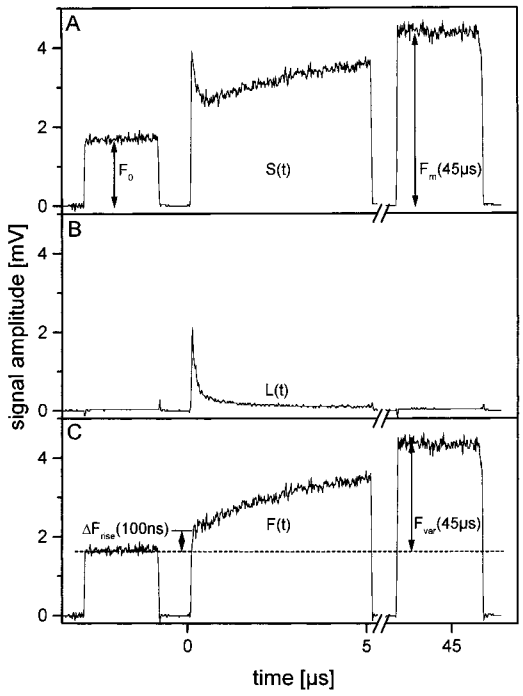

FIGURE 1: Time course of fluorescence emission signals before and after excitation of thylakoid suspensions with a saturating actinic laser flash and the measuring LED beam switched on (panel A) or turned off (panel B), respectively. Curve C is the difference of curves A and B. These curves are averages of 80 measurements.

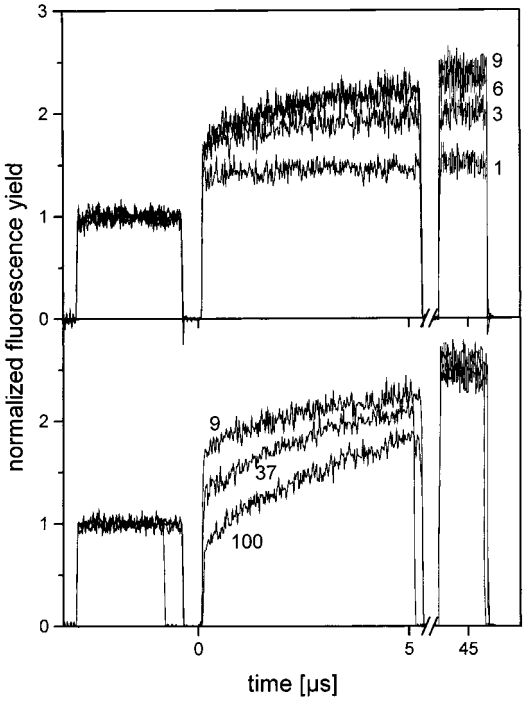

FIGURE 2: Time course of normalized fluorescence quantum yield of dark-adapted thylakoid suspensions before and after an actinic laser flash of different energies. The curves represent the differences between traces monitored when the measuring light beam is on or off, respectively (see panel C of Figure 1). The numbers labeling the curves describe the relative energies related to the maximum laser pulse energy that is set to 100%.

The data collected before and after each laser flash was transferred via a GPIB-bus (PC IIA, National Instruments) to a computer. The sample cuvette was flushed and refilled after each series of eight laser flashes with a computer controlled home-built flow system. To improve the signal-to-noise ratio 80 measurements of series of eight laser flashes were averaged.

RESULTS AND DISCUSSION

Flash-Induced Fluorescence Changes in Thylakoids. Figure 1 shows typical traces induced by a single actinic flash in dark-adapted thylakoid suspensions when signals are monitored with the measuring beam of the LED array either switched on (panel A) or turned off (panel B) during the measurement. In the top panel, the signal F_0 before the actinic flash is entirely due to the fluorescence emission caused by the weak measuring beam. It reflects the normalized fluorescence quantum yield Φ_o^{rel} of dark-adapted PS II complexes, because the fluorescence emitted by the sample is generally given by the relation

$$F = c\Phi I_{measuring} \quad (1)$$

where c is a constant (its value depends on the optical geometry of the setup), Φ is the fluorescence quantum yield and $I_{measuring}$ the light intensity of the LED array that is absorbed by the sample.

The signal/noise ratio increases with progressing intensity of the measuring light beam. However, increased $I_{measuring}$ gives rise to enhanced excitation of PS II. Therefore, $I_{measuring}$ has to be limited and optimal measuring conditions selected. A useful check for the absence of an actinic effect by the measuring beam is a constant zero level in the absence of an actinic laser flash. It has always been checked that F_0 remains virtually independent of illumination time with the LED measuring beam. This feature indicates that $I_{measuring}$ is below the level of detectable interfering actinic effects by the monitoring light. An independent test is the measure of the period four oscillation of the extent of nanosecond-kinetics as a function of the measuring beam intensity as will be outlined in the Results and Discussion. The results obtained confirm that the actinic effect of $I_{measuring}$ used in this study is negligibly small (see Figure 6A).

During the time interval where the gate of the MCP-PMT is turned off, a saturating actinic laser flash hitting the sample at $t = 0$ transfers within 1 ns all PS II complexes into the "stable" charge separation state $P680^{\bullet+}PheoQ_A^{\bullet-}$ (*6*−*8*). After the gate is switched on (at $t = 100$ ns after the actinic flash), the MCP-PMT monitors a transient signal S(t). It is characterized by an "instantaneous" rise followed by a rapid decline and subsequent slower rise kinetics. At about 45 μs after the actinic flash, a maximum level symbolized by F_m-(45 μs) is reached. At saturating intensity of the actinic laser flash, the ratio of $F_m(45\ \mu s)/F_0$ is about 2.7, which is typical for the flash-induced increase of the relative fluorescence quantum yield (*14*, *28*). It is slightly lower (by about 20%) than values reported recently for the F_m/F_0 ratio of 3.2 measured at a delay of 100 μs (*14*, *28*) because at 45 μs the slow rise components with lifetimes of the order of 30 μs are not completed.

A striking feature of the traces in Figure 1 is the rapid transient in the nanosecond time domain. A phenomenon comparable with that of $S(t)$ has been reported in ref *24* for the first flash but has never been observed in other studies because it escaped detection owing to limited time resolution of equipment (*14*, *25*). At a first glance, the spike of $S(t)$ in

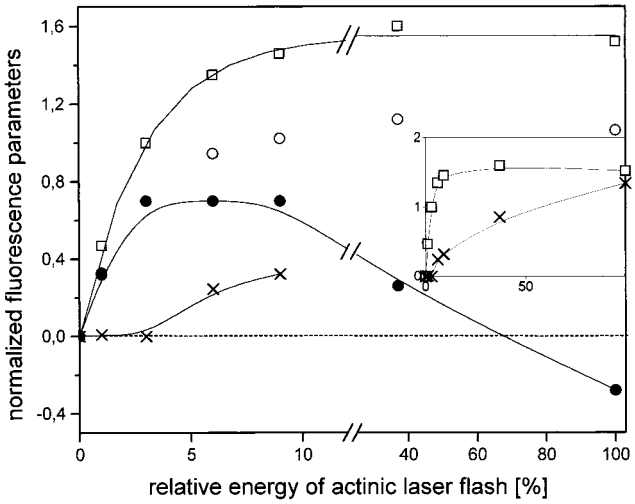

FIGURE 3: Dependence on relative laser flash energy (E^{rel}_{flash}) of $\Delta F_V(45\ \mu s)/F_O$ (open squares), $\Delta F^{exp}_{rise}(100\ ns)/F_O$ (filled circles), $\Delta F^{calc}_{rise}(100\ ns)/F_O$ (open circles) and $\Delta F(^3Car)/F_O$ (crosses) in dark-adapted thylakoids excited with a single actinic flash. The data were gathered from the experimental traces shown in Figure 2. In the main figure, the E^{rel}_{flash} scale is enlarged in the 0−10% region, the inset shows the full linear scale.

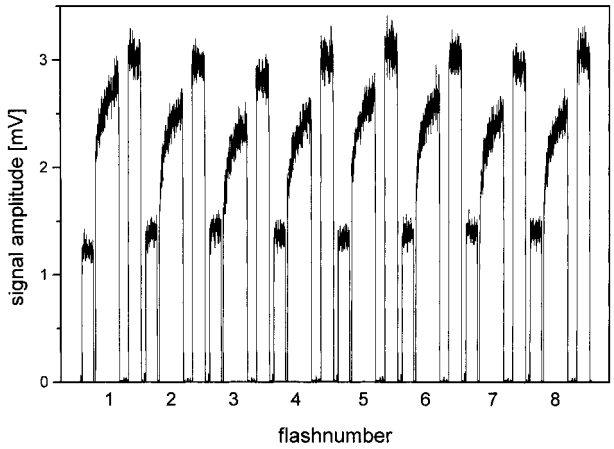

FIGURE 4: Time course of flash-induced changes of relative fluorescence quantum yield in thylakoid suspensions excited by a train of eight actinic laser flashes at 1 Hz and $E^{rel}_{flash} = 9\%$. The traces obtained as difference of signals measured with the LED beam turned on or off, respectively (see Figure 1, panel C), represent the average of 80 measurements.

the ns time domain appears to be surprising. Since $I_{measuring}$ is kept constant during the measurements, $F(t)$ is expected to be directly proportional to $\Phi(t)$ (see eq *1*) and therefore the ratio $F(t)/F_0$ provides a measure of the relative quantum yield $\Phi^{rel}(t)$. Accordingly, a continuous rise is expected due to the removal of the fluorescence quencher $P680^{\bullet+}$ through its reduction by Y_Z. A closer inspection reveals that part of the "instantaneous" rise and the subsequent rapid decline of signal $S(t)$ in panel A of Figure 1 are not reflecting changes of the relative fluorescence quantum yield $\Phi^{rel}(t)$ because this feature symbolized by $L(t)$ is also observed when the measuring beam is turned off as is shown in panel B. In this case ($I_{measuring} = 0$) the signals F_0 and F_m are zero (see panel B). The transient signal $L(t)$ cannot originate from the prompt fluorescence caused by the strong actinic flash because the lifetime of this emission is a few nanoseconds only (*3*, *4*), and therefore, any of its contributions are negligible at a delay

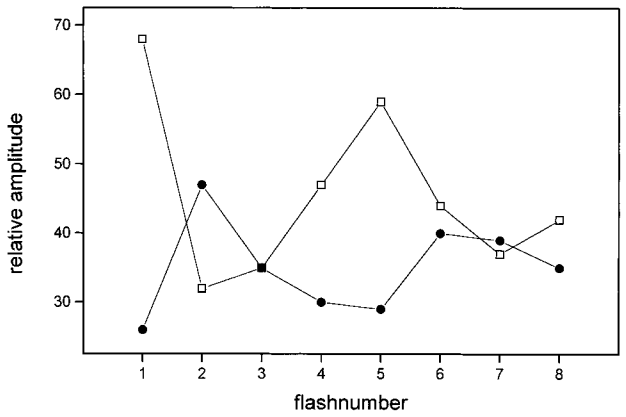

FIGURE 5: Normalized extent of "fast" (open squares) and "slow" (filled circles) ns components of $P680^{\bullet+}$ reduction as a function of flash number in dark-adapted spinach thylakoids. The normalized extent ascribed to ^3Car decay is independent of flash number with $a_3 = 0.32$ (see Figure 3). The results were obtained by a numerical fit to eq 2 of the experimental data depicted in Figure 4. For further details see text.

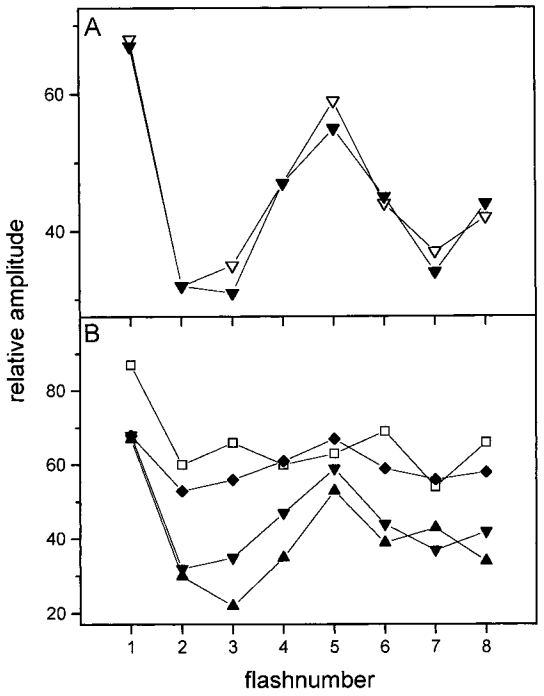

FIGURE 6: Normalized amplitudes $a_1(n)$ as a function of flash number monitored either at constant E^{rel}_{flash} and two different measuring beam intensities $I_{measuring}$ (panel A) or at constant $I_{measuring}$ and different E^{rel}_{flash} values (panel B). In panel A, open and closed symbols represent measurements at normally used $I_{measuring}$ and at a value increased by factor 1.7, respectively; $E^{rel}_{flash} = 9\%$. In panel B, the symbols describe measurements at normal $I_{measuring}$ and E^{rel}_{flash} values of 1% (open squares), 3% (closed triangles), 9% (inverted closed triangles), and 37% (closed diamonds).

time of 100 ns. The signal $L(t)$ in panel B might either reflect an artifact due to distortion of the detector system or rapid components of delayed light emission. To address this problem, the wavelength dependence of the amplitude of $L(t)$ was analyzed. It was found that the signal exhibits a spectrum which corresponds with that of the prompt fluorescence of chlorophyll in thylakoids (see Figure 2 of ref *29*). Furthermore, amplitude and kinetics of $L(t)$ were shown to depend on the redox state S_i of the WOC. Accordingly, the observed transient $L(t)$ is ascribed to fast components of delayed

fluorescence as outlined in ref *29*. A comparable phenomenon has been reported in a former study (*24*) where the fluorescence yield due to a probe pulse was found to decay when its delay increases from 200 to 500 ns with respect to a strong actinic pump pulse. In contrast to our observation, this decay was only observed after the first but not after the fourth flash of a train of actinic laser pulses (*24*). Therefore, the particular "first flash phenomenon" described in the above-mentioned report is difficult to explain and artifacts due to a monitoring blue flash of about 700 ns FWMH cannot be excluded.

The results of panel B illustrate that the new equipment in a suitable operating mode (i.e., turning off the LED array during the measurement) offers for the first time the possibility to study delayed light emission in the nanosecond time domain after excitation of PS II with saturating laser flashes (*29*). A more detailed study on the properties of fast components of delayed fluorescence in different sample types is beyond the scope of this study and will be outlined in a forthcoming paper.

Flash-Induced Changes of Relative Fluorescence Yield at High Time Resolution. To extract the time course of the flash-induced fluorescence yield, i.e., $F(t)$, from the signals $S(t)$ obtained in the presence of the measuring light beam (panel A), the signals of panel B have to be subtracted. It has to be emphasized that the measuring light beam does not exert a detectable actinic activity (vide supra) so that $F(t)$ is not affected. The difference obtained is shown in panel C. It reveals that the actinic flash gives rise to the expected monotonic increase of the relative fluorescence quantum yield. The overall rise exhibits two characteristics: (i) a kinetically unresolved "instantaneous" increase (within a 100 ns time resolution) symbolized by $\Delta F_{rise}(100\ ns)$ and (ii) subsequent multiphasic kinetics. The rise kinetics of the normalized fluorescence quantum yield reflect the superposition of time-dependent populations of different quenchers. Within a time domain of 45 μs after the actinic laser flash, the rise kinetics are expected to be dominated by two reactions: reduction of $P680^{\bullet+}$ with Y_Z as donor and turnover of carotenoid triplets (^{3}Car), as outlined in more detail in ref *11*.

The reduction of $P680^{\bullet+}$ by Y_Z in PS II complexes with intact WOC is multiphasic with a pronounced 20−50 ns kinetics of a normalized extent that exhibits a characteristic period four oscillation (*12*−*14*). Accordingly, this component gives rise to an "instantaneous" rise at 100 ns time resolution. This rise is counterbalanced by a decrease owing to formation of carotenoid triplets, which are well-known to act as fluorescence quenchers (*30*−*32*). A recent analysis with solubilized LHC II has shown that triplet−triplet energy transfer from ^{3}Chl to Car is faster than 1 ns (*33*). Accordingly, ^{3}Car formation is limited by intersystem crossing at Chl, which takes place within about 10 ns. The populations of states $P680^{\bullet+}Q_A^{\bullet-}$ and ^{3}Car are not linearly related because they exhibit drastically different dependencies on the energy of the actinic laser flash. The onset of ^{3}Car formation corresponds with light saturation of photosynthesis and then strongly increases with progressing flash intensity in both green plants (*34*) and purple bacteria (*35*, *36*). As a consequence, the "instantaneous" change of the fluorescence yield symbolized by $\Delta F_{rise}(100\ ns)$ (see Figure 1) is expected to exhibit a characteristic dependence on the energy of the actinic laser flash (E_{flash}). At subsaturating levels of photosynthesis, the contribution of ^{3}Car quenching is virtually negligible (*34*, *35*), and the amplitude of the "instantaneous" rise should increase with progressing E_{flash}. However, in the low energy region the S_i-state transition probability is smaller and the period four oscillation in a flash sequence affected. Therefore, saturating flashes should be used when analyzing the S_i-state dependence. On the other hand, when reaching a saturation level, the extent of $P680^{\bullet+}Q_A^{\bullet-}$ remains constant but the ^{3}Car population steeply increases with E_{flash}. As a result, the extent of the "instantaneous" rise decreases and eventually completely disappears and even turns into a net "instantaneous" decrease of $\Delta F_{rise}(100\ ns)$. To check for this phenomenon and to optimize the experimental conditions, measurements were performed at different actinic laser flash intensities. In this respect, it is important to note that in dark-adapted thylakoids the WOC almost completely populates the redox state S_1 (*37*, *38*) and therefore the reaction after the first flash at different energies is not affected by the WOC.

Flash-Induced Changes of Relative Fluorescence Yield as a Function of Energy of the Actinic Laser Flash. The results obtained at different E_{flash}-values are shown in Figure 2. In the following, the maximum flash energy (see Materials and Methods) will be set to 100% and all E_{flash} values given as percentage of this value. These relative energies are symbolized by E^{rel}_{flash}. The traces on the top panel measured with comparatively weak actinic laser flashes exhibit the expected increase of the amplitude of the "instantaneous" rise $\Delta F_{rise}(100\ ns)$ with increasing E^{rel}_{flash} values. This feature mainly reflects saturation of $P680^{\bullet+}Q_A^{\bullet-}$ formation and reduction of $P680^{\bullet+}$ by Y_Z via the "fast" ns kinetics (vide supra). The effect of progressing population of ^{3}Car and the concomitant quenching effect are clearly seen by the traces in the bottom panel of Figure 2. The extent of the $\Delta F_{rise}(100\ ns)/F_O = \Phi^{rel}_{rise}(100\ ns)$ decreases with increasing E^{rel}_{flash} and turns into the opposite direction at highest E^{rel}_{flash} values. To illustrate the counterbalancing effect in more detail, it is necessary to separate the effect due to photochemical saturation of $P680^{\bullet+}Q_A^{\bullet-}$ formation from the E_{flash} dependence of ^{3}Car population. When dark-adapted thylakoids are excited with a single flash, most of the $P680^{\bullet+}$ is reduced by Y_Z after a dark time of 45 μs while the majority of $Q_A^{\bullet-}$ still remains reduced (for further discussion, see ref *11*) and all ^{3}Car acting as quencher disappeared with a lifetime of about 2−5 μs under aerobic conditions (*33*, *39*). Accordingly, the flash-induced change at 45 μs, $F_m(45\ \mu s) - F_O = F_V(45\ \mu s)$, normalized to F_O can be used as a measure of the saturation behavior of PS II complexes with an intact WOC. The data (open squares) presented in Figure 3 reveal that the level of $F_V(45\ \mu s)/F_O = \Phi^{rel}_V(45\ \mu s)$ as a function of E^{rel}_{flash} reaches almost complete saturation when E^{rel}_{flash} is about 10%.

At low E^{rel}_{flash} values, a similar increase as for $\Phi^{rel}_V(45\ \mu s)$ is observed for the extent of $\Phi^{rel}_{rise}(100\ ns)$, but at higher intensities, drastic deviation arise (filled circles in Figure 3).

When normalizing the values of $\Phi^{rel}_V(45\ \mu s)$ and $\Phi^{rel}_{rise}(100\ ns)$ to the corresponding data measured at $E^{rel}_{flash} = 3\%$, the expected saturation of $\Phi^{rel}_{rise}(100\ ns)$ owing to $P680^{\bullet+}$ reduction by Y_Z can be obtained. Accordingly, the difference

between these "calculated" $\Phi^{rel}_{rise}(100\ ns)_{calc}$ values and the measured $\Phi^{rel}_{rise}(100\ ns)_{exp}$ data provides an estimation of the quenching effect of ^{3}Car. This difference denoted as $\Delta\Phi(^3Car)$ is a measure of the ^{3}Car population because in a recent detailed analysis a linear correlation was found to exist between fluorescence quenching and ^{3}Car population in solubilized LHC II (*40*). The inset of Figure 3 compares the E^{rel}_{flash} dependencies of $\Phi^{rel}_V(45\ \mu s)$ and $\Delta\Phi(^3Car)$ over the whole E^{rel}_{flash} range in a linear scale. The results of Figure 3 are in perfect agreement with previous findings, indicating that the onset of ^{3}Car formation corresponds with photochemical closing of reaction centers of PS II (*34*) and purple bacteria (*35*). It has to be emphasized that this analysis provides a fully consistent qualitative picture but it does not permit detailed quantitative conclusions owing to the approximations that are used. Especially the properties of parameter $\Phi^{rel}_V(45\ \mu s)$ as a measure of PS II activity has to be discussed because it can only be considered as a useful quantitative approach if the fraction of PS II complexes with an intact WOC is sufficiently high. Otherwise, slower kinetics of $P680^{\bullet+}$ reduction in PS II lacking a competent WOC could significantly affect the $\Phi^{rel}_V(45\ \mu s)$ level. The influence of PS II heterogeneity is of special relevance for the exact shape of the saturation curves if the antenna size of different types of PS II complexes exhibit marked variations. A latest report based on fluorescence measurements with much lower time resolution (2−3 orders of magnitude compared with the present study) revealed that PS II complexes with different stages of functional competence readily exhibit a pronounced lateral heterogeneity within the thylakoid membranes (*41*).

Changes of Relative Fluorescence Yield in Dark-Adapted Thylakoids Excited with a Train of Eight Actinic Laser Flashes. To investigate period four oscillations as a characteristic "fingerprint" for the turnover of the redox states S_i in the WOC, suspensions of dark-adapted thylakoids from spinach were excited with a train of eight saturating laser flashes. On the basis of the results described in Figures 2 and 3, this experiment was performed with $E^{rel}_{flash} = 9\%$. Figure 4 shows the flash-induced fluorescence changes as difference of signals monitored with the measuring light beam either switched on or turned off (see Figure 1C). An inspection of Figure 4 reveals two striking features: (i) the rise kinetics of $F(t)$ exhibits a typical period four oscillation with pronounced contributions after the first and fifth flash, and (ii) the $F_m(45\ \mu s)$ levels also oscillate with maxima after the first and fifth flash, whereas F_0 prior to each actinic flash is smaller for the first flash and varies only slightly in the following flashes with a maximum after the third flash.

The dependence of F_0 on the flash number n is in perfect agreement with previous findings observed in suspensions of chlorella cells (*42*). Likewise, the oscillation pattern of $F_m(45\ \mu s)$ qualitatively corresponds with former reports (*14*, *42*, *43*), but it is less pronounced at about 45 μs (present study) compared with that of the maximum fluorescence levels measured a few hundred milliseconds after each saturating actinic flash (*42*, *43*). These general properties of F_0 and $F_m(45\ \mu s)$ in samples with an intact WOC are well-known variations (*42*, *43*) and will not be discussed here.

The most interesting feature of the traces in Figure 4 are the rise kinetics of $F(t)$ induced by saturating laser flashes. The time resolution achieved with the newly developed equipment permits for the first time a separation of the fluorescence rise in the ns time domain into a "fast" and "slow" component and to determine their period four oscillation patterns. For kinetic fits, the data is normalized to the difference $F_m(45\ \mu s) - F_0$ caused by the first actinic flash. According to eq 1, these data reflect the flash-induced normalized fluorescence yield Φ^{rel} with $\Phi^{rel}_o(1) = 0$ and $\Phi^{rel}_m(1) = 1$. A deconvolution of the data monitored in the time window of 100 ns to 5 μs was performed by a numerical fit to the formula

$$\Phi^{rel}(t) = \sum_{i=1}^{2} a_i[1 - \exp(-t/\tau_i)] - a_3 \exp(-t/\tau_3) \quad (2)$$

where $\sum_{i=1}^{2} a_i = \Phi^{rel}_m - \Phi^{rel}_o = \Phi^{rel}_V$ is normalized to 1; the indices $i = 1$ and 2 are used for the "fast" and "slow" ns component of $P680^{\bullet+}$ reduction by Y_Z. The value τ_1 for the "fast" ns rise component is fixed to 30 ns because this part of the kinetics cannot be resolved at a "dead time" of about 100 ns (it has been checked that replacing the fixed time of 30 ns by either 20 or 40 ns does not affect the general pattern). Furthermore, the lifetime τ_3 of ^{3}Car acting as fluorescence quencher is assumed to be 5 μs under our experimental conditions (*33*, *39*) and the extent of ^{3}Car formation (a_3) in each flash is expected to be virtually independent of the redox state S_i of the WOC. The extent of a_3 is gathered from the difference $\Delta\Phi(^3Car)$ shown in Figure 3. The contribution of the 35 μs kinetics of $P680^{\bullet+}$ reduction by Y_Z due to relaxation processes (*11*, *14*, *16*, *28*) is comparatively small and can be neglected in the time domain of $\leq 5\ \mu$s.

A numerical fit of the experimental data of Figure 4 to eq 2 within the framework of the above-mentioned assumptions leads to results that are depicted in Figure 5. An inspection of the dependencies on the flash number n readily shows that the amplitudes $a_1(n)$ and $a_2(n)$ both exhibit a characteristic period four oscillation but of opposite direction, i.e., $a_1(n)$ attains pronounced maximum values after the first and fifth flash where $a_2(n)$ has the smallest amplitudes, while $a_1(n)$ exhibits minima after the second and third flash where $a_2(n)$ reaches maxima. This feature perfectly corresponds with the results gathered from a deconvolution of the relaxation kinetics of 830 nm absorption changes induced by a train of saturating laser flashes in dark-adapted PS II membranes from spinach (*12*, *13*). Therefore, the present study provides the first direct evidence that the S_i-state dependence of the extent of "fast" and "slow" nanosecond components of the flash-induced fluorescence rise is the same as that of $P680^{\bullet+}$ reduction by Y_Z. This finding offers the possibility to use the noninvasive fluorescence methods for studying $P680^{\bullet+}$ reduction kinetics in whole cells (vide infra).

Oscillation Patterns of Fast Nanosecondns Rise at Different Measuring Light Intensities and Flash Energies. With respect to the results in Figure 4, another important point has to be addressed. The oscillation patterns of $a_1(n)$ and $a_2(n)$ exhibit the characteristic features of $P680^{\bullet+}$ reduction but the redox transition $S_i \rightarrow S_{i+1}$ of the WOC within the Kok-cycle (*42*) might be desynchronized by two effects: (i) the measuring light beam could exert a significant actinic effect thereby leading to further advancement of the S_i-state transitions, and (ii) subsaturating actinic laser flashes should

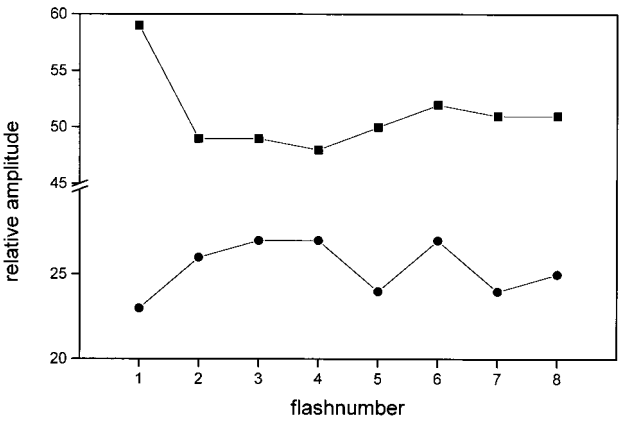

FIGURE 7: Normalized extent of the "fast" (closed squares) and "slow" (closed circles) ns components of $P680^{\bullet+}$ reduction kinetics in dark-adapted cells of *Chlamydomonas reinhardtii*. The normalized extent ascribed to ^{3}Car decay is independent of flash number with $a_3 = 0.86$ (data not shown). The results were obtained by a numerical fit to eq 2 of experimental data measured analogously as in thylakoids (see Figure 5) but at $E^{rel}_{flash} = 37\%$. For further details see text.

give rise to an additional contribution to the intrinsic probability of misses. To check for both possibilities the oscillation patterns were measured and analyzed for (i) constant E^{rel}_{flash} but $I_{measuring}$ that differs by a factor of about 1.7., and (ii) different E^{rel}_{flash} values at constant measuring light intensity $I_{measuring}$.

The values of $a_1(n)$ gathered from the experimental data are compiled in Figure 6. The traces in panel A reveal that the oscillation pattern remains nearly unaffected by almost doubling of $I_{measuring}$, i.e., an actinic effect by the measuring LED beam can be excluded under the experimental conditions used in this study. Panel B shows the effect of E^{rel}_{flash} on the period four oscillation. Significant changes are only observed at an E^{rel}_{flash} value of 1%. At a first glance, the latter finding is somewhat surprising because the dependence of $F_m(45\ \mu s)$ on the actinic flash intensity exhibits only a saturation degree of about 65% at $E^{rel}_{flash} = 3\%$ (see Figure 3). One interesting conclusion emerging from this finding is the idea that all PS II complexes with an intact WOC and $P680^{\bullet+}$ reduction by Y_Z via "fast" nanosecond-kinetics are more easily to saturate by light than the total population of PS II. This phenomenon can be rationalized by the assumption that the former complexes are connected with a larger antenna system. The possible relation with the recently described lateral heterogeneity of different types of PS II within the thylakoid membrane (*41*) and physiological implications have to be analyzed in future investigations.

Oscillation Pattern of the Extent of Nanosecond Kinetics in Chlamydomonas Cells. To illustrate the potential of the new equipment for noninvasive studies of $P680^{\bullet+}$ reduction via "fast" nanosecond-kinetics in whole cells, analogous experiments as described in Figure 4 for isolated spinach thylakoids were performed with suspensions of the green algae *Chlamydomonas reinhardtii*. The results obtained were analyzed by using eq 2 and analogous assumptions for the "fast" nanosecond component and the decay of ^{3}Car as described for thylakoids. The results obtained and summarized in Figure 7 readily show that the oscillation patterns of $a_1(n)$ and $a_2(n)$ resemble those of thylakoids from spinach. This finding indicates that the dependence of $P680^{\bullet+}$ reduction kinetics on the redox states S_i of the WOC is a general property of PS II. To the best of our knowledge this is the first report on the oscillation pattern of $P680^{\bullet+}$ reduction by Y_Z in intact cells. It shows that the new fluorometic method opens the road for in vivo analyses of the very fast $P680^{\bullet+}$ turnover. A closer inspection reveals quantitative differences (phase shift by one flash) that are ascribed to physiological properties. These details are beyond the scope of this study. Preliminary experiments reveal that the technique can also be successfully used for studies of $P680^{\bullet+}$ reduction in whole leaves.

ACKNOWLEDGMENT

The authors would like to thank Dr. Heike Witt for providing the *Chlamydomonas reinhardtii* cells and the members of the electronic and mechanical workshop at the Max-Volmer-Institute for technical help in construction of the experimental setup.

REFERENCES

1. Papageorgiou, G. (1975) in *Bioenergetics of Photosynthesis* (Govindjee, Ed.) pp 319−371, Academic Press, New York.
2. Murata, N., and Satoh, K. (1986) in *Light Emission by Plants and Bacteria* (Govindjee, Amesz, J., and Fork, D. C., Eds.) pp 137−159, Academic Press, Orlando.
3. Renger, G., Eckert, H.-J., Bergmann, A., Bernarding, J., Liu, B., Napiwotzki, A., Reifarth, F., and Eichler, H.-J. (1995) *Austr. J. Plant Physiol. 22*, 167−181.
4. Roelofs, T. A., Lee, C. H., and Holzwarth, A. R. (1992) *Biophys. J. 61*, 1147−1163.
5. Bergmann, A., Eichler, H.-J., Eckert, H.-J., and Renger, G. (1999) *Photosynth. Res. 58*, 305−312.
6. Nuijs, A. M., van Gorkom, H. J., Plijter, J. J., and Duysens, L. M. N. (1986) *Biochim. Biophys. Acta 848*, 167−172.
7. Eckert, H.-J., Wiese, N., Bernarding, J., Eichler, H.-J., and Renger, G. (1988) *FEBS Lett. 240*, 153−158.
8. Bernarding, J., Eckert, H.-J., Eichler, H. J., Napiwotzki, A., and Renger, G. (1994) *Photochem. Photobiol. 59*, 566−573.
9. Butler, W. L. (1972) *Proc. Natl. Acad. Sci. U.S.A. 69*, 3420−3422.
10. Duysens, L. M. N., and Sweers, H. E. (1963) *Microalgae and Photosynthetic Bacteria*, pp 353−372, University of Tokyo Press, Tokyo.
11. Christen, G., Seeliger, A., and Renger, G. (1999) *Biochemistry 38*, 6082−6092.
12. Brettel, K., Schlodder, E., and Witt, H. T. (1984) *Biochim. Biophys. Acta 766*, 403−415.
13. Eckert, H.-J., and Renger, G. (1988) *FEBS Lett. 236*, 425−431.
14. Christen, G., and Renger, G. (1999) *Biochemistry 38*, 2068−2077.
15. Hays, A. M., Vassiliev, I. R., Golbeck, J. H., and Debus, R. J. (1999) *Biochemistry 38*, 11851−11865.
16. Schilstra, M. J., Rappaport, F., Nugent, J. H. A., Barnett, C. J., and Klug, D. R. (1998) *Biochemistry 37*, 3974−3981.
17. Reinman, S., and Mathis, P. (1981) *Biochim. Biophys. Acta 635*, 249−258.
18. Renger, G., Völker, M., and Weiss, W. (1984) *Biochim. Biophys. Acta 766*, 582−591.
19. Robinson, H. H., and Crofts, A. R. (1983) *FEBS Lett. 153*, 221−226.
20. Weiss, W., and Renger, G. (1984) in *Advances in Photosynthesis Research* (Sybesma, C., Ed.) Vol. 1, pp 167−170, Martinus Nijhoff/Dr. W. Junk Publishers, Den Haag.
21. Schreiber, U. (1986) *Photosynth. Res. 9*, 261−272.
22. Govindjee (1995) *Austr. J. Plant Physiol. 22*, 131−160.
23. Joliot, P., and Kok, B. (1975) in *Bioenergetics of Photosynthesis* (Govindjee, Ed.), pp 387−412, Academic Press, New York.

24. Mauzerall, D. (1972) *Proc. Natl. Acad. Sci. U.S.A. 69*, 1358−1362.
25. Reifarth, F., Christen, G., and Renger, G. (1997) *Photosynth. Res. 51*, 231−242.
26. Winget, G. D., Izawa, S., and Good, N. E. (1965) *Biochem. Biophys. Res. Commun. 21*, 438−443.
27. Harris, H. E. (1988) *The Chlamydomonas Sourcebook*, Academic Press, San Diego.
28. Christen, G., Reifarth, F., and Renger, G. (1998) *FEBS Lett. 429*, 49−52.
29. Christen, G., Steffen, R., and Renger, G. (2000) *FEBS Lett. 475*, 103−106.
30. Breton, J., Geacintov, N. E., and Swenberg, C. E. (1979) *Biochim. Biophys. Acta 548*, 616−635.
31. Lavorel, J., and Etienne, A. L. (1977) in *Primary Processes of Photosynthesis* (Barber, J., Ed.) pp 203−268, Elsevier, Amsterdam.
32. Mathis, P., Butler, W. L., and Satoh, K. (1979) *Photochem. Photobiol. 30*, 603−614.
33. Schödel, R., Irrgang, K.-D., Voigt, J., and Renger, G. (1998) *Biophys. J. 75*, 3143−3153.
34. Wolff, C., and Witt, H. T. (1972) in *Primary Processes of Photosynthesis* (Barber, J., Ed.) Vol. 2, pp 931−936, Elsevier, Amsterdam.
35. Renger, G., and Wolff, C. (1977) *Biochim. Biophys. Acta 460*, 57−67.
36. Monger, T. G., Cogdell, R. J., and Parson, W. W. (1976) *Biochim. Biophys. Acta 449*, 136−153.
37. Vermaas, W. C. J., Renger, G., and Dohnt, G. (1984) *Biochim. Biophys. Acta 764*, 194−202.
38. Messinger, J., and Renger, G. (1993) *Biochemistry 32*, 9379−9386.
39. Siefermann-Herms, D., and Angerhofer, A. (1998) *Photosynth. Res. 55*, 83−94.
40. Schödel, R., Irrgang, K.-D., Voigt, J., and Renger, G. (1999) *Biophys. J. 76*, 2238−2248.
41. Mamedov, F., Stefansson, H., Albertsson, P.-A., and Styring, S. (2000) *Biochemistry 39*, 10478−10486.
42. Delosme, R. (1972) in *Photosynthesis, two centuries after its discovery by Joseph Priestly* (Forti, G., Avron, M., and Melandri, A., Eds.) Vol. 1, pp 187−195, De. W. Junk Publishers, The Hague, The Netherlands.
43. Joliot, P., and Joliot, A. (1972) in *Primary Processes of Photosynthesis* (Barber, J., Ed.) Vol. 2, pp 931−936, Elsevier, Amsterdam.

BI0011779